

TAUP 2721/2003  
DESY 03-011  
hep-ph/ 0302010

# $J/\psi$ Photo- and DIS Production via Nonlinear Evolution

E. Gotsman <sup>a 1)</sup>, E. Levin <sup>a, b 2)</sup>, M. Lublinsky <sup>b 3)</sup>, U. Maor <sup>a 4)</sup> and E. Naftali <sup>a 5)</sup>

<sup>a)</sup> *School of Physics and Astronomy  
Raymond and Beverly Sackler Faculty of Exact Science  
Tel Aviv University, Tel Aviv, 69978, ISRAEL*

<sup>b)</sup> *DESY Theory Group  
22603, Hamburg, GERMANY*

## Abstract:

We apply our solution of the nonlinear evolution equation to the case of  $J/\psi$  photo and DIS production on nucleons and nuclei targets. The uncertainty in the  $J/\psi$  wave function normalization due to Fermi motion is treated as a free parameter. We obtain good reproduction of the HERA experimental data on a proton target. Calculations of  $J/\psi$  mesons coherent production on nuclei targets are presented and discussed. Our analysis supports the conclusions reached in our previous studies, stressing the importance of nonlinear evolution in the kinematical domain of high-density QCD.

---

1) gotsman@post.tau.ac.il

2) leving@post.tau.ac.il

3) lublinm@mail.desy.de

4) maor@post.tau.ac.il

5) erann@post.tau.ac.il

# 1 Introduction

It was recognized long ago [1] that the interactions of virtual photons at high-energies and low virtualities are governed by nonlinear evolution. Over the years, different theoretical methods of calculating processes in the kinematical region of high-density QCD (hdQCD) have been proposed [2, 3, 4, 5, 6, 7], leading to the construction of an equation, which incorporates both linear evolution due to parton splitting, and nonlinear evolution due to the recombination of partons at high-density. This equation is given in Eq. (1) below, using the notations of [7], for  $\tilde{N}(r_\perp, x; b)$ , the imaginary part of the amplitude of a dipole of size  $r_\perp$ , which scatters elastically at impact parameter  $b$ .

In this paper we extend our recent investigations [8, 9] of the nonlinear evolution to vector mesons, focusing on  $J/\psi$  photo [10] and DIS [11] production. As this process is characterized by a scale of the order of the charmed quark mass,  $m_c$ , it is considered a primary candidate for investigating the kinematical region of QCD on the boundary between perturbative and hdQCD.

In our previous publications [12, 13] we demonstrated that the cross section experimental data for  $J/\psi$  production is well reproduced if one employs two damping factors, calculated using a Glauber like shadowing-correction (SC) formalism [14]. Broadly speaking, each damping factor may be considered as one iteration in an iterative procedure for determining  $\tilde{N}(r_\perp, x; b)$ . These iterations correspond to Glauber rescatterings where the first iteration is attributed to SC due to the passage of a dipole through the target, and the second iteration is attributed to one small  $x$  gluon emitted by the dipole prior to the interaction. We believe that the SC formalism was, at the time, an important preliminary step towards the more rigorous treatment of [9].

A particular outcome of [13], is that the  $J/\psi$  experimental data for the forward differential cross section slope,  $B$ , can be well reproduced by assuming that the profile function in the impact parameter space is the Fourier transform of an electromagnetic dipole-like form factor. Our numerical calculations of  $B$  produced a satisfactory fit to the experimental data with a hadron radius  $R^2 = 10 \text{ GeV}^{-2}$ . On the other hand, in [9], a good fit to the  $F_2$  data was obtained with  $R^2 = 3.1 \text{ GeV}^{-2}$  for an exponential form factor, and  $R^2 = 4.5 \text{ GeV}^{-2}$ , for a dipole-like form factor. We consider the radii in [9] as effective radii which are reduced due to (i) the presence of inelastic diffractive processes; and (ii) the observation that in the simple expression typically used for  $\sigma_{\text{dipole}}$ , the dipole-proton cross section, a small anomalous dimension has been assumed. As we shall see, when calculating the cross section for  $J/\psi$  production, it is necessary to include an effective  $b$ -dependence, which we choose to extract from the HERA experimental data.

This paper is organized as follows: in section 2 we briefly review the nonlinear equation and the approximate numerical solution to it, as obtained in [9]; in section 3 we calculate the integrated cross section for  $J/\psi$  photo- and DIS- production, and compare to the relevant

experimental data; in section 4 we present our predictions for the production of  $J/\psi$  from scattering of electrons on heavy nuclei. Our summary and conclusions are given in section 5.

## 2 The Dipole Scattering Amplitude

The imaginary part of the dipole scattering amplitude,  $\tilde{N}$ , is a solution of a nonlinear evolution equation, which characterizes the low  $x$  behavior of the parton densities, while taking into account hdQCD effects, thereby obeying the unitarity constraints. The equation describes the interaction with a target of a parent dipole, of size  $\mathbf{x}_{01}$ , and of two dipoles, of sizes  $\mathbf{x}_{12}$  and  $\mathbf{x}_{02}$ , which were produced by the dipole of size  $\mathbf{x}_{01}$ . The probability for the decay of the dipole of size  $\mathbf{x}_{01}$  is given by the square of its wave function, which, in a simplified form, can be written as  $x_{01}^2/x_{02}^2 x_{12}^2$ .

Each of the produced dipoles can interact with the target independently, with respective amplitudes of  $\tilde{N}(\mathbf{x}_{12}, y; \mathbf{b} - \frac{1}{2}\mathbf{x}_{02})$  and  $\tilde{N}(\mathbf{x}_{02}, y; \mathbf{b} - \frac{1}{2}\mathbf{x}_{12})$ , where  $y$  denotes the rapidity variable and  $b$  the impact parameter. However, adding these contributions clearly overestimates the dipole-nucleon interaction, since one must consider the probability that during the interaction, one dipole is in the shadow of the other. This negative correction factor is given by  $-\tilde{N}(\mathbf{x}_{12}, y; \mathbf{b} - \frac{1}{2}\mathbf{x}_{02})\tilde{N}(\mathbf{x}_{02}, y; \mathbf{b} - \frac{1}{2}\mathbf{x}_{12})$ .

Thus,  $\tilde{N}$  can be written in the form

$$\begin{aligned} \tilde{N}(\mathbf{x}_{01}, Y; b) = & \tilde{N}(\mathbf{x}_{01}, Y_0; b) \exp \left[ -\frac{2 C_F \alpha_s}{\pi} \ln \left( \frac{\mathbf{x}_{01}^2}{\rho^2} \right) (Y - Y_0) \right] + \\ & \frac{C_F \alpha_s}{\pi^2} \int_{Y_0}^Y dy \exp \left[ -\frac{2 C_F \alpha_s}{\pi} \ln \left( \frac{\mathbf{x}_{01}^2}{\rho^2} \right) (Y - y) \right] \times \\ & \int_{\rho} d^2 \mathbf{x}_2 \frac{\mathbf{x}_{01}^2}{\mathbf{x}_{02}^2 \mathbf{x}_{12}^2} \left( 2 \tilde{N}(\mathbf{x}_{02}, y; \mathbf{b} - \frac{1}{2}\mathbf{x}_{12}) - \tilde{N}(\mathbf{x}_{02}, y; \mathbf{b} - \frac{1}{2}\mathbf{x}_{12}) \tilde{N}(\mathbf{x}_{12}, y; \mathbf{b} - \frac{1}{2}\mathbf{x}_{02}) \right), \end{aligned} \quad (1)$$

where,  $Y = -\ln x$ ,  $Y_0 = -\ln x_0$  and  $\rho$  is an ultraviolet cutoff, which does not appear in the physical quantities.

The linear part of (1) is the LO BFKL equation [15], which describes the evolution of the multiplicity of the fixed size color dipoles as a function of the energy  $Y$ . The equation sums the high twist contributions. Note, that the linear part of (1) also has higher twist contributions and the main contribution of the nonlinear part is to the leading twist (see [2] for general arguments and [16] for explicit calculations).

For completeness, we provide a brief description of the steps taken in [9] for obtaining an approximate solution for  $\tilde{N}(\mathbf{x}_{01}, Y; b)$ .

The initial conditions for (1) were taken at  $x_0 = 10^{-2}$  in the eikonal approximation, accounting for multiple dipole-target interactions:

$$\tilde{N}(\mathbf{x}_{01}, x_0; b) = 1 - e^{-\frac{1}{2}\sigma_{\text{input}}(\mathbf{x}_{01}, x_0) S(b)}, \quad (2)$$

where

$$\sigma_{\text{input}}(\mathbf{x}_{01}, x_0) = \frac{\alpha_s \pi^2}{N_c} x_{01}^2 x G^{\text{DGLAP}}(x_0, 4/x_{01}^2), \quad (3)$$

and  $S(b)$  is the profile function in impact parameter space. As stated, we found that the experimental data of the differential cross section slope,  $B$ , is well described by the following profile function, which is the Fourier transform of electromagnetic dipole-like form factor:

$$S(b) = \frac{2}{\pi R^2} \frac{\sqrt{8}b}{R} K_1\left(\frac{\sqrt{8}b}{R}\right). \quad (4)$$

As a first step, the  $b$ -dependence of (1) was neglected. Thus, all twist contributions for the evolution were summed, using the initial condition (2) at  $b = 0$ . Then, once an approximate solution was obtained, the  $b$  dependence is restored, assuming similar  $b$ -dependences for both the solution and the initial conditions. Specifically, the following ansatz was used for the  $b$ -dependence of  $\tilde{N}$ :

$$\tilde{N}(r_\perp, x; b) = (1 - e^{-\kappa(x, r_\perp) S(b)/S(0)}), \quad (5)$$

where

$$\kappa(x, r_\perp) = -\ln(1 - \tilde{N}(r_\perp, x, b = 0)). \quad (6)$$

### 3 Cross section for $J/\psi$ production

The cross section for  $J/\psi$  production is given by:

$$\sigma(\gamma^* p \longrightarrow V p) = \int d^2b \left| \int dz d^2r_\perp \Psi_{\gamma^*}(r_\perp, z, Q^2) \mathcal{A}(r_\perp, x; b) \Psi_V(r_\perp, z) \right|^2, \quad (7)$$

where  $\mathcal{A}(r_\perp, x; b)$  is the imaginary part of the production amplitude in impact parameter space, and  $\Psi_V$  and  $\Psi_{\gamma^*}$  are, respectively, the wave functions of the  $J/\psi$  and the virtual photon. Formally speaking  $\Psi_V$  should depend on  $b$ . However, as the dominant contribution of the  $J/\psi$  wave function comes from short distances, this dependence is neglected. The evaluation of (7) is done by first performing the polarization summation of the  $J/\psi$ -photon overlap function,  $\Psi_V \times \Psi_{\gamma^*}$ . This overlap function can be derived in the  $r_\perp$  representation using the spin structures of the vector meson wave function [17] and the well-known photon wave function [18].

A detailed analysis of the overlap function has already been made in [19], where it was found that, in the momentum representation, the overlap function for transverse (T) and longitudinal (L) polarized photon is given by [19]:

$$\Psi_V(k_\perp, z) \times \Psi_{\gamma^*, T}(k_\perp, z) \propto \frac{2(z^2 + (1-z)^2)k_\perp^2 a^2 + m_c^2(a^2 - k_\perp^2)}{m_c(a^2 + k_\perp^2)^3} \Psi_V(k_\perp, z), \quad (8)$$

$$\Psi_V(k_\perp, z) \times \Psi_{\gamma^*, L}(k_\perp, z) \propto \frac{2z(1-z)Q(a^2 - k_\perp^2)}{(a^2 + k_\perp^2)^3} \Psi_V(k_\perp, z), \quad (9)$$

with  $a^2 = z(1-z)Q^2 + m_c^2$ . Here  $\times$  denotes the polarization and helicity summation. For a given  $J/\psi$  spatial distribution, the transformation to configuration space is straightforward and is given in Eqs. (10)–(11) below. Although many models exist for the spatial distributions of vector mesons (see for example, [17, 20, 21, 22, 23, 24]), we choose to approximate  $\Psi_V(r_\perp, z)$  to be  $\Psi_V(r_\perp = 0, z = \frac{1}{2})$ . As in our previous publications [12, 13], we consider below a deviation from this approximation due to relativistic effects, produced by the Fermi motion of the bound quarks within the vector meson.

The effect of this motion, however, strongly depends on the charmed quark mass,  $m_c$ . If one assumes, for example, that  $m_c = M_\psi/2 \simeq 1.55$  GeV, then, by definition, there is no correction due to Fermi motion. On the other hand, in [20], it has been assumed that  $m_c \simeq 1.50$  GeV, and a suppression factor of the cross section of about 0.25 was obtained, with almost no energy dependence. Hence, as it stands, the contribution of this effect lies within a substantial range of uncertainty in which  $m_c$  varies by no more than 0.05 GeV.

We, therefore, consider the effect of Fermi motion as an uncertainty of the wave function normalization, introducing it as an overall (energy-independent) suppression factor,  $K_F$ , which we use as a fitting parameter. Using the above approximation we Fourier transform Eqs. (8) and (9) and obtain:

$$\Psi_V(r_\perp = 0, z = \frac{1}{2}) \times \Psi_{\gamma^*, T}(r_\perp; Q^2) = \frac{K_F}{48\alpha_{\text{em}}} \sqrt{\frac{3\Gamma_{ee}M_\psi}{\pi}} \times \left\{ \frac{a^2}{m_c} \left( \zeta K_1(\zeta) - \frac{\zeta^2}{4} K_2(\zeta) \right) + m_c \left( \frac{\zeta^2}{2} K_2(\zeta) - \zeta K_1(\zeta) \right) \right\} \quad (10)$$

$$\Psi_V(r_\perp = 0, z = \frac{1}{2}) \times \Psi_{\gamma^*, L}(r_\perp; Q^2) = \frac{K_F}{48\alpha_{\text{em}}} \sqrt{\frac{3\Gamma_{ee}M_\psi}{\pi}} \frac{Q}{2} \left( \frac{\zeta^2}{2} K_2(\zeta) - \zeta K_1(\zeta) \right). \quad (11)$$

where  $\zeta = ar_\perp$ ,  $K_i, i = 1, 2$  are the modified Bessel functions and  $\Gamma_{ee} = 5.26$  KeV is the leptonic width of the  $J/\psi$ .

Before presenting our results for the cross section (7), we discuss the impact parameter dependence of the production amplitude,  $\mathcal{A}$ . At first sight,  $\mathcal{A}(r_\perp, x; b)$  equals  $\tilde{N}(r_\perp, x; b)$  where its  $b$ -dependence is related to the solution of Eq. (1) at  $b = 0$  through the ansatz of Eq. (5). The

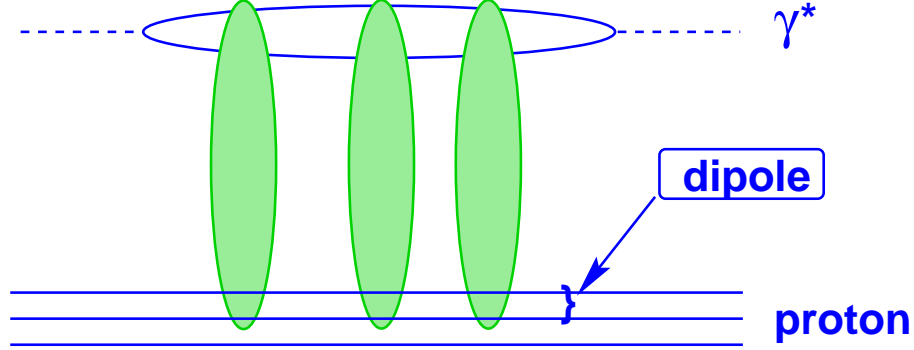


Figure 1: Rescatterings for total DIS cross section.

parameter  $R$  in  $S(b)$  [see Eq. (4)] is related to the hadron size and has already been determined in [9] by fitting  $\tilde{N}$  to the experimental data of  $F_2$ . However, as stated in the introduction, a good fit to  $F_2$  was obtained using a relatively small value of  $R^2 = 4.5 \text{ GeV}^2$ , whereas we know that the the measured  $J/\psi$  differential slope,  $B$ , is consistent with a radius which is more than twice larger.

Hence, it turns out that  $\mathcal{A}$  differs from  $\tilde{N}$ . The correct  $b$ -dependence of  $\mathcal{A}$  is given by the following expression:

$$\mathcal{A}(r_{\perp}, x; b) = \int d^2b' \tilde{N}(r_{\perp}, x; b') S'(b - b'). \quad (12)$$

To understand Eq. (12) we need to recall the procedure for calculating the total cross section for the deep inelastic process which is shown in Fig. 1. If one uses the specific model in which the proton consists of two colour dipoles (see Refs. [25, 26] for details), the total deep inelastic cross section is given solely by the scattering amplitude of one particular dipole present in the proton target. More specifically, as there is no momentum transfer which is involved in the process, the total cross section does not depend on the probability of finding a second (spectator) dipole in the target.

On the other hand, in the process of  $J/\psi$  production, the momentum transfer,  $q$ , is not zero (see Fig. 2). In this process, for fixed momentum transfer, the  $t = -q^2$  dependence of the  $J/\psi$  production relates both to  $\tilde{N}(r_{\perp}, x; q)$  (the amplitude for the photon to scatter off one dipole) and to the probability to find the second dipole having a momentum  $q$  inside of the recoiled proton. Denoting this probability by  $S'(q)$ , the production amplitude is thus proportional to  $\tilde{N}(r_{\perp}, x; q)S'(q)$ . A product in momentum representation is equivalent to a convolution in the impact parameter, hence the form of Eq. (12).

Actually, we can estimate  $S'(q)$  using the Born approximation for the scattering amplitude shown in the diagram of Fig. 3. Assuming a simple factorized form of the proton wave function,

$$\Psi_{\text{proton}}(r_{\perp}, \rho_{\perp}) = \phi(r_{\perp}) \phi(\rho_{\perp}) \quad (13)$$

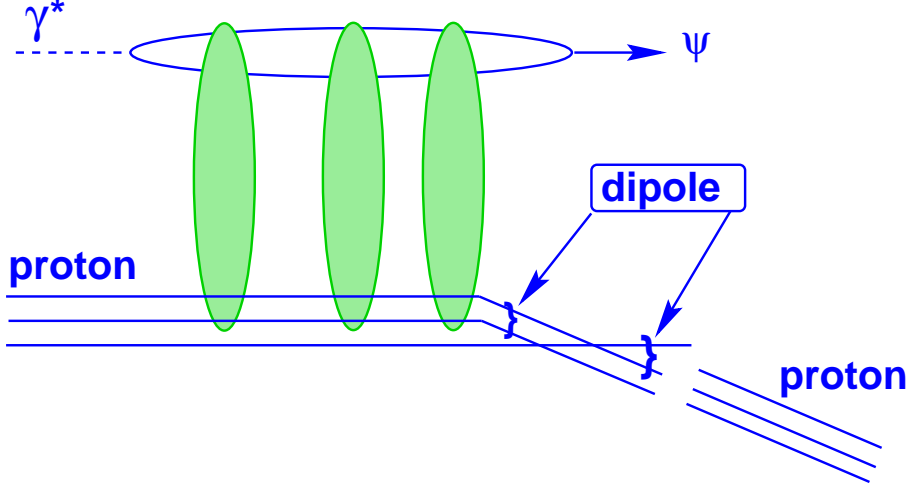


Figure 2: Rescatterings for  $J/\psi$  cross section at fixed  $t = -q^2$ .

where  $\rho_{\perp} = r_{1,\perp} - r_{2,\perp}$  and  $r_{\perp} = r_{3,\perp} - (r_{1,\perp} + r_{2,\perp})/2$ , we can easily calculate  $S'(q)$

$$S'(q) = \int d^2 r_{\perp} |\phi(r_{\perp})|^2 e^{i\frac{1}{3}\vec{q}r_{\perp}} \quad (14)$$

Comparing Eq. (14) with the expression for the electromagnetic form factor for proton

$$F(q) = \int d^2 r_{\perp} |\phi(r_{\perp})|^2 e^{i\frac{2}{3}\vec{q}r_{\perp}} \quad (15)$$

one can see that  $S'(b)$  can be described by Eq. (4) with  $R = R_{\text{proton}}/2$ , where  $R_{\text{proton}}$  is the electromagnetic radius of proton.

Alternatively, we can choose a different strategy and extract the typical size for the profile function  $S'(b)$  using the experimental data. Generally, the differential slope is related to the average of the square of impact parameter, weighted by the the dipole-proton cross section. The correct averaging procedure would be to integrate both over the impact parameter and over the dipole size, thereby reconstructing the energy dependence of  $B$  (the shrinkage of the diffraction peak):

$$B(x) = \frac{1}{2}\langle b^2 \rangle = \frac{\int d^2 r_{\perp} b^2 d^2 b \tilde{N}(r_{\perp}, x, b)}{2 \int d^2 r_{\perp} d^2 b \tilde{N}(r_{\perp}, x, b)}. \quad (16)$$

The value of  $B$  as obtained from (16) is, of course, not universal for all processes, and it directly depends on the choice of  $S(b)$ . For the purpose of calculating the effective radius to be used in  $S'(b)$ , we define the deviation of  $\frac{1}{2}\langle b^2 \rangle$  from the measured slope to be:

$$B' = B_{\text{exp}} - \frac{1}{2}\langle b^2 \rangle, \quad (17)$$

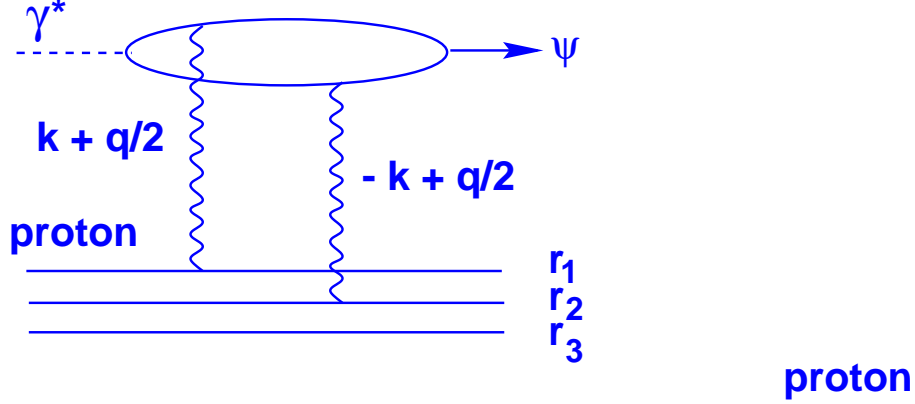


Figure 3: The amplitude in the Born approximation for the  $J/\psi$  cross section at fixed  $t = -q^2$ .

where,  $B_{\text{exp}}$  is taken from experimental data (see, *e.g.*, [27]).  $S'(b)$  is then calculated from Eq. (4) with the substitution  $R \rightarrow R' = 2B'$ .

The resulting  $b$ -dependence of  $\mathcal{A}(x; b) \equiv \int d^2r_{\perp} \mathcal{A}(r_{\perp}, x; b) \Psi_{\gamma}(r_{\perp}) \Psi_V$  are shown in Fig. 4. The convolution of  $S'(b)$  with  $\tilde{N}(r_{\perp}, x; b')$  is realized by a shift in the maximum of the scattering amplitude in the impact parameter space. The decrease of the amplitude in the low  $b$  region may be understood as a signature of shadowing corrections needed to insure unitarity.

Our calculations of  $\sigma(\gamma^* p \rightarrow J/\psi)$  were basically in accordance with Eq. (7), with modifications due to the contribution from the real part of the production amplitude [28] and the skewed (off diagonal) gluon distribution [29]. The contribution of the real part is given by:

$$C_R^2 = (1 + \rho^2), \quad (18)$$

where,

$$\rho = \text{Re}\mathcal{A}/\text{Im}\mathcal{A} = \text{tg}\left(\frac{\pi\lambda}{2}\right) \quad (19)$$

and, in our approach,

$$\lambda = \partial \ln(\tilde{N}) / \partial \ln\left(\frac{1}{x}\right). \quad (20)$$

Note that with this definition of  $\lambda$ , its value obeys the unitarity constraint according to which, at a fixed value of  $Q^2$ ,  $\lambda$  is a decreasing function of the energy with  $\lambda \rightarrow 0$  as  $x \rightarrow 0$  [9].

The off diagonal contribution is given by:

$$C_G^2 = \left( \frac{2^{2\lambda+3} \Gamma(\lambda + \frac{5}{2})}{\sqrt{\pi} \Gamma(\lambda + 4)} \right)^2. \quad (21)$$

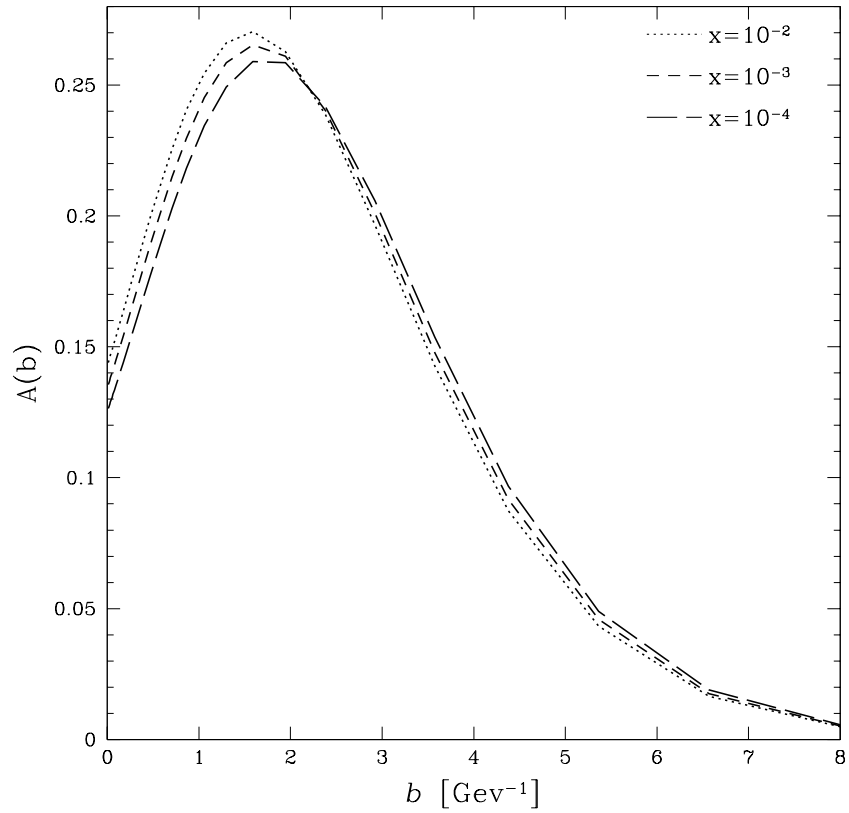


Figure 4: The impact parameter dependence of the  $J/\psi$  production amplitude.

Formally, the definition (20) of  $\lambda$  is  $r_\perp$ -dependent. In practice, the corrections due the  $r_\perp$ -dependence of  $\lambda$  are rather small. Thus,  $\lambda$  is computed at fixed scale  $r_\perp^2 = 4/(Q^2 + M_{J/\psi}^2)$ .

The results of our calculations of Eq. (7), given the above modifications, are shown in Fig. 5 for  $J/\psi$  photoproduction, where we define  $x = M_{J/\psi}^2/W^2$ . We found that the H1 data [30] are compatible with  $K_F = 0.6$  ( $\chi^2/\text{n.d.f.} = 0.5$ ) while the ZEUS data require  $K_F = 0.76$  ( $\chi^2/\text{n.d.f.} = 0.6$ ). As stated, the factor  $K_F$  is the deviation of our approximation for the  $J/\psi$  static potential wave function from a more realistic model, in which the spatial distribution of  $J/\psi$  depends on  $r_\perp$  and  $z$ . Our results are consistent with [24], where a comparison between a realistic and static  $J/\psi$  wave functions was made.

The values of  $K_F$  which were obtained for  $Q^2 = 0$ , were used to predict the cross section for  $Q^2 > 0$ . In Fig. 6 we compare the  $Q^2 > 0$  predictions to the preliminary data which were read off plots in [11]. Within the experimental errors, our reproduction of the data is good, except for data at  $Q^2 = 16 \text{ GeV}^2$  where we underestimate the H1 point ( $W \simeq 80 \text{ GeV}$ ) and one of the ZEUS points ( $W \simeq 180 \text{ GeV}$ ). In spite of this, the overall  $\chi^2/\text{n.d.f.}$  for photoproduction and DIS data (including these two problematic points) is 0.73 for ZEUS and 0.84 for H1.

## 4 Predictions for Heavy Nuclei

In this section we assess the unitarity effects in  $J/\psi$  coherent production in photo and DIS on a nuclear target. In such processes, unitarity effects are more pronounced than in  $e-p$  collisions. Thus, with nuclear targets one can access the region of hdQCD at values of  $x$  which are larger than those characterizing this region at HERA experiments.

The production of vector mesons on a nuclear target can be calculated in a straightforward manner using methods similar to the above. In principle, (1) can be solved separately for each atomic number  $A$ , with the same form of initial conditions. To this end we choose to present our predictions using the Glauber approach, and for the time being to postpone the solution of (1) for nuclei.

In the Glauber approach, the cross-section for the  $J/\psi$  production, including contributions for the percolation through a nucleus of both a  $|q\bar{q}\rangle$  system and a  $|q\bar{q}g\rangle$  system, is given by the following expression:

$$\sigma(\gamma^* A \longrightarrow J/\psi A) = \int d^2b \left| \int dz d^2r_\perp \Psi_{\gamma^*}(r_\perp, z, Q^2) \Psi_{J/\psi}(r_\perp, z) \times \left[ \left(1 - e^{-\frac{1}{2}\Omega_q}\right) + \frac{C_F}{\pi^2} \alpha_s r_\perp^2 \int \frac{dx}{x} \int_{r'_\perp > r_\perp} \frac{d^2r'_\perp}{r'^4_\perp} \left(1 - e^{-\frac{1}{2}\Omega_g}\right) \right] \right|^2, \quad (22)$$

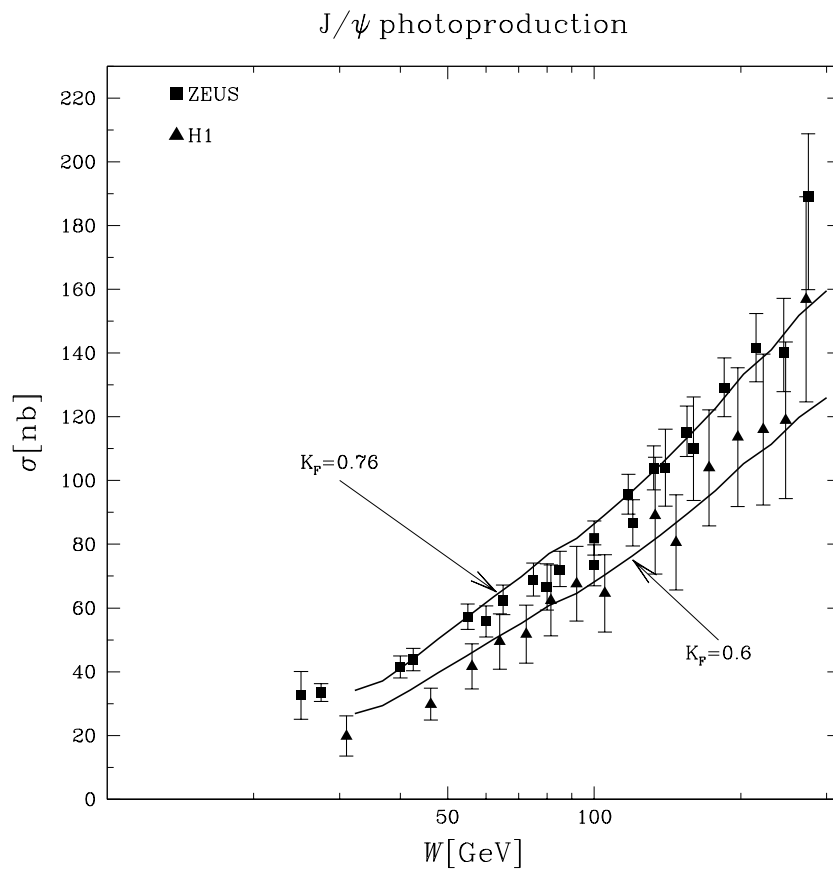


Figure 5: The ZEUS and H1  $J/\psi$  photoproduction data compared with our calculations using NLE.

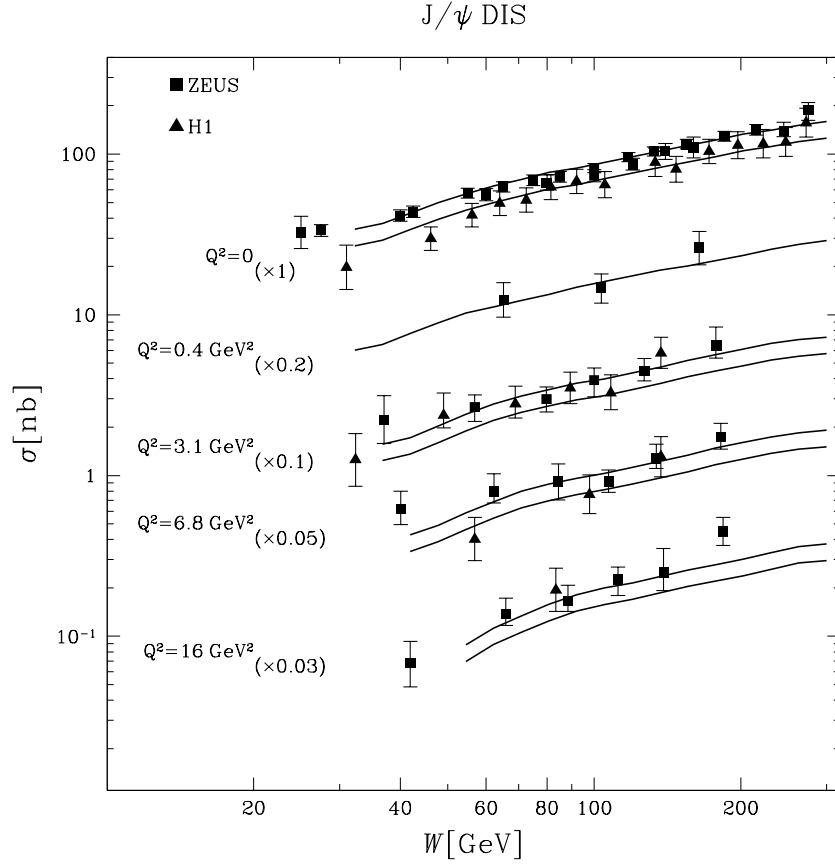


Figure 6:  $J/\psi$  DIS and photoproduction, data and our calculations using NLE. The upper (lower) curves at each  $Q^2$  bin correspond to different  $K_F$  values, which were fitted to ZEUS (H1) photoproduction data.

where the opacities  $\Omega_q$  and  $\Omega_g$  are defined as:

$$\Omega_q(b, r_\perp, x) = \frac{\pi^2}{3} r_\perp^2 \alpha_s \left( \frac{4}{r_\perp^2} \right) xG \left( x, \frac{4}{r_\perp^2} \right) S_A(b), \quad (23)$$

$$\Omega_g(b, r_\perp, x) = \frac{9}{4} \Omega_q(b, r_\perp, x), \quad (24)$$

$S_A(b)$  is the number of nucleons in a nucleus interacting with the incoming dipole and  $xG$  is the gluon density obtained from linear DGLAP evolution (we used CTEQ parameterization [31] for this particular computation).

We are cognisant of the fact that when dealing with heavy nuclei interactions, neither a dipole nor a Gaussian are adequate for  $S_A(b)$ . When the probing hadronic system percolates through a heavy nucleus, it experiences multiple rescatterings over a substantially long region of the impact parameter space. On the other hand, once the system leaves the heavy nuclei, the number of strong interactions decreases rapidly.

Our approach is to use the Wood-Saxon parameterization [32] for the impact parameter dependence,  $S_A(b)$ :

$$S_A(b) = \rho \int \frac{dr_\parallel}{1 + e^{\frac{r - R_A}{h}}} \quad (25)$$

where  $r_\parallel$  is the longitudinal distance from the target,  $h$  and  $R_A$  are parameters which are taken from experimental tables [33],  $r = \sqrt{r_\parallel^2 + b^2}$  and the normalization factor  $\rho$  is defined in the following relation:

$$\rho \int \frac{dr_\parallel d^2b}{1 + e^{\frac{r - R_A}{h}}} = A. \quad (26)$$

Note that  $R_A$  is associated with the radius of a nucleus with atomic number  $A$ .

To determine the variance between nuclei targets and a nucleon target, we need to examine the  $A$  dependence of the integrated cross section, by comparing the calculated cross section to a power behaviour of  $\sigma \propto A^\delta$ . The maximal value of the exponent,  $\delta_{max}$ , depends on the profile function  $S_A(b)$ , and can be found from the following integral:

$$A^{\delta_{max}} = \int d^2b |S_A(b)|^2 \quad (27)$$

For an exponential profile,  $\delta_{max} = \frac{4}{3}$  and for a Wood-Saxon profile of (25),  $\delta_{max} \approx 1.43$ . A deviation from the maximal value of  $\delta$  would be a clear signature of saturation of the growth of the cross section. Fig. 7a shows the cross section as a function of  $A$  with an arbitrary normalization, for  $x = 10^{-5}, 10^{-4}$  and  $10^{-3}$ . To illustrate the saturation effect, we compare the curves to a power behavior of  $\sigma \propto A^{4/3}$ . Unitarity conserving effects are already appreciable at  $x = 10^{-3}$ .

Eq. (22) takes into account the interaction of the quark-antiquark pair and the fastest gluon. On the other hand, we can improve our Glauber approach by using the solution of the non-linear equation, since the solution to the non-linear equation takes into account all possible interactions of partons with the nucleon target. As stated,  $R_p^2$ , the effective radius of nucleon turns out, in our approach, to be very small. With such a small radius, the typical parameter that governs the dipole interaction with the nuclear target is also very small, namely,

$$R_p^2 S_A(0) \leq 1. \quad (28)$$

In the standard approach, however,  $R_p^2 S_A(0)$  was considered to be large. We thus have to take into account all rescatterings inside the proton in the first stage of our approach and treat the interactions with different nucleons in a nucleus using the Glauber formula.

Specifically, the cross section can be written in the form:

$$\sigma(\gamma^* A \longrightarrow J/\psi A) = \int d^2b \left| \int dz d^2r_\perp \Psi_{\gamma^*}(r_\perp, z, Q^2) \Psi_{J/\psi}(r_\perp, z) \left( 1 - e^{-\frac{1}{2}\sigma(\text{dipole-nucleon})S_A(b)} \right) \right|^2 \quad (29)$$

where  $\sigma(\text{dipole} - \text{nucleon})$  is equal to  $2 \int d^2b N(r^2, x; b)$  where  $N$  is dipole-nucleon amplitude.

The following figures illustrate the effect of the inclusion of all rescatterings. Fig. 7b shows the cross section of Eq. (29) as a function of  $A$  with an arbitrary normalization, for  $x = 10^{-5}, 10^{-4}$  and  $10^{-3}$ .

In Fig. 7c we display the characteristic exponent,  $\delta$ , as a function of  $x$ , for the calculated cross-sections of Eqs. (22) and (29). The upper curve in Fig. 7c corresponds to the numerical calculation of Eq. (29) and the lower curve corresponds to Eq. (22). In terms of  $\delta$ , the differences between the two approaches are negligible. On the other hand, as further detailed below, there is a considerable normalization difference.

To investigate the normalization difference, we define the following ratio:

$$\mathcal{R} = \frac{\text{Eq. (29)}}{\text{Eq. (22)}} \quad (30)$$

We have calculated  $\mathcal{R}$  for  $J/\psi$  photoproduction on a Gold target ( $A \simeq 200$ ). The results, as a function of the energy, for several values of  $Q^2$ , are shown in Fig. 7d. Our calculations show that the full calculation is suppressed by a factor of about 0.4 with respect to the calculation in which only a  $|q\bar{q}\rangle$  and a  $|q\bar{q}g\rangle$  systems are considered to interact with the nucleus.

Our prediction for the energy dependence for  $J/\psi$  production on a Gold target, in the calculation which includes all parton interactions is shown in Fig. 8 for several values of  $Q^2$ . In this figure, we have used the wave function normalization which we have extracted from the data on proton target. Due to the uncertainty of this normalization, and to the 0.4 ratio of Eq. (30), our rough estimation of the relative errors of the curves are of the order of 15-20% .

### J/ $\psi$ on nuclei

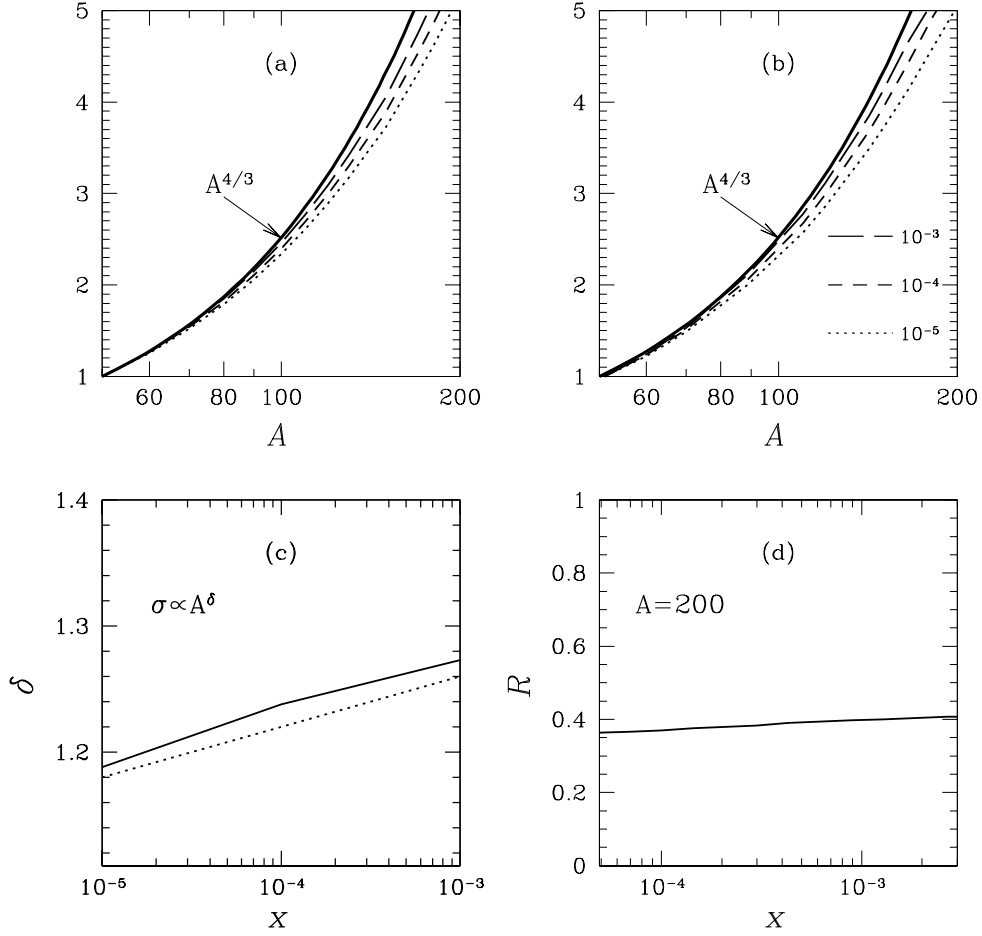


Figure 7:  $J/\psi$  photoproduction on a nuclear target: (a)-(b) show the  $A$ -dependence of the cross section for different values of  $x$ , normalized to unity at  $A = 50$  [(a) shows the contribution due to the interactions of  $|q\bar{q}\rangle$  and  $|q\bar{q}g\rangle$  with the nucleus, and (b) shows the contributions of all interactions]; (c) shows the values of  $\delta$ , as a function of  $x$ , where the lower curve corresponds to plot (a) and the upper curve corresponds to plot (b); and (d) shows the normalization ratio between plot (a) and plot (b) as explained in the text.

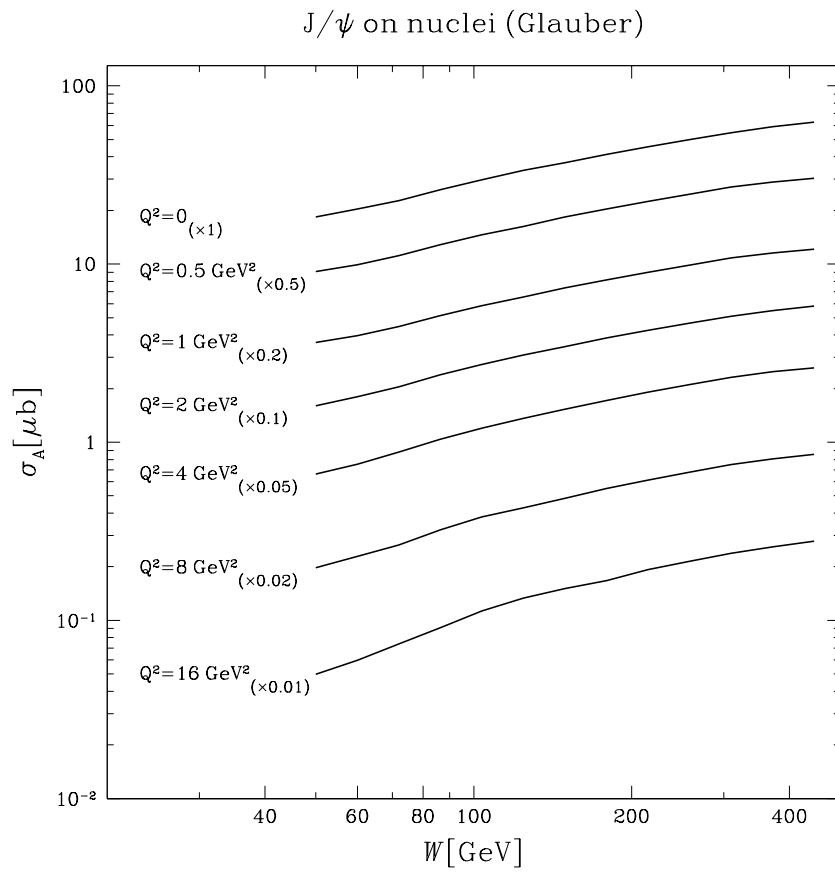


Figure 8: Predictions for  $J/\psi$  photo- and DIS production on a Gold target, using the Glauber approach of Eq. (29) for different values of  $Q^2$  as a function of  $W$ .

## 5 Summary

We have extended our recent investigation of the approximate solution of the nonlinear evolution equation to the case of  $J/\psi$  photo- and DIS production. We have convoluted our previous ansatz for the  $b$ -dependence of the amplitude with an additional profile which is extracted from the electromagnetic form factor. The resulting impact parameter dependence of the amplitude exhibits a decrease near  $b = 0$ . We believe that this decrease is due to the deviation from the linear evolution equations, and is a signature for the onset of unitarity taming effects.

We have used the solution to the NLE and obtained a satisfactory reproduction of both the photo- and the DIS production data. Our free parameter was the uncertainty in the  $J/\psi$  wave function normalization due to Fermi motion of the  $c\bar{c}$  pair. In addition, we took into account modifications of the cross section due to the real part of the amplitude and the existence of skewed gluons within the nucleon.

We used the Glauber approach to calculate the cross section for  $J/\psi$  production on a nuclear target. Our predictions demonstrate that such processes are important for the understanding of unitarity taming effects. We have found that these effects start to dominate for  $x \leq 10^{-3}$ . Hence, the predictions presented here may be verified with the future eRHIC experiments.

It is important to note that, apart from the uncertainties due to vector meson wave function, the calculations on nuclei do not contain any fitting parameters. More specifically the uncertainty due to  $b$  dependence of the solution for nuclei is quite small. In other words, the initial conditions for the BK equation [6, 7] are determined solely by the proton DIS data.

## Acknowledgments

**This paper is dedicated to our friend and colleague Jan Kwiecinski on the occasion of his sixty-fifth birthday, may he continue to be active and contribute for many years to come.**

Two of us (E.G. and E.L.) thank the DESY Theory Division for their hospitality. This research was supported in part by GIF grant # I-620-22.14/1999 and by Israeli Science Foundation, founded by the Israeli Academy of Science and Humanities.

## References

- [1] L. V. Gribov, E.M. Levin and M.G. Ryskin, *Phys. Rep.* **100** (1983) 1.
- [2] A. H. Mueller and J. Qiu, *Nucl. Phys.* **B268** (1986) 427

- [3] L. McLerran and R. Venugopalan, *Phys. Rev.* **D49** (1994) 2233; 3352; **D 50** (1994) 2225, **D 53** (1996) 458, **D 59** (1999) 094002.
- [4] E. Levin and M.G. Ryskin, *Phys. Rep.* **189** (1990) 267;  
 J. C. Collins and J. Kwiecinski, *Nucl. Phys.* **B 335** (1990) 89;  
 J. Bartels, J. Blumlein, and G. Shuler, *Z. Phys.* **C 50** (1991) 91;  
 A. L. Ayala, M. B. Gay Ducati, and E. M. Levin, *Nucl. Phys.* **B 493** (1997) 305, **B 510** (1990) 355;  
 Yu. Kovchegov, *Phys. Rev.* **D 54** (96) 5463, **D 55** (1997) 5445, **D 61** (2000) 074018;  
 A. H. Mueller, *Nucl. Phys.* **B 572** (2000) 227, **B 558** (1999) 285;  
 Yu. V. Kovchegov, A. H. Mueller, *Nucl. Phys.* **B 529** (1998) 451; E. Iancu, A. Leonidov, and L. McLerran, *Nucl. Phys.* **A 692** (2001) 583; M. Braun, *Eur. Phys. J.* **C 16** (2000) 337.
- [5] J. Jalilian-Marian, A. Kovner, L. McLerran, and H. Weigert, *Phys. Rev.* **D55** (1997) 5414; J. Jalilian-Marian, A. Kovner, and H. Weigert, *Phys. Rev.* **D 59** (1999) 014015; J. Jalilian-Marian, A. Kovner, A. Leonidov, and H. Weigert, *Phys. Rev.* **D 59** (1999) 034007, Erratum-ibid. *Phys. Rev.* **D 59** (1999) 099903; A. Kovner, J. Guilherme Milhano, and H. Weigert, *Phys. Rev.* **D 62** (2000) 114005; *Nucl. Phys.* **A 703** (2002) 823.
- [6] Ia. Balitsky, *Nucl. Phys.* **B 463** (1996) 99.
- [7] Yu. Kovchegov, *Phys. Rev.* **D 60** (2000) 034008.
- [8] M. Lublinsky, E. Gotsman, E. Levin, and U. Maor, *Nucl. Phys.* **A696** (2001) 851.
- [9] E. Gotsman, E. Levin, M. Lublinsky and U. Maor, hep-ph/0209074.
- [10] ZEUS Collaboration, S. Chekanov *et al.* *Eur. Phys. J.* **C24** (2002) 345
- [11] ZEUS Collaboration, contribution No. 813 to the XXXIst Int. conf. on HEP, 24-21 July, 2002, Amsterdam, The Netherlands.
- [12] E Gotsman, E.M Levin, U. Maor, E Ferreira and E Naftali, *Phys. Lett.* **B503** (2001) 277.
- [13] E. Gotsman, E. Levin, U. Maor and E. Naftali, *Phys. Lett.* **B503** (2001) 277.
- [14] E. Gotsman, E. Levin and U. Maor, *Phys. Lett.* **B425** (1998) 369; E. Gotsman, E. Levin, U. Maor and E. Naftali, *Nucl. Phys.* **B539** (1999) 535.
- [15] E. A. Kuraev, L. N. Lipatov, and F. S. Fadin, *Sov. Phys. JETP* **45** (1977) 199; Ya. Ya. Balitsky and L. N. Lipatov, *Sov. J. Nucl. Phys.* **28** (1978) 22 .
- [16] J. Bartels, K. Golec-Biernat and K. Peters, *Eur. Phys. J.* **c17** (2000) 121; E. Gotsman, E. Levin, U. Maor, L. McLerran, and K. Tuchin, *Nucl. Phys.* **A683** (2001) 383; *Phys. Lett.* **B506** (2001) 289.

- [17] S. J. Brodsky, L. Frankfurt, J. F. Gunion, A. H. Mueller and M. Strikman, *Phys. Rev.* **D50** (1994) 3134.
- [18] A. H. Mueller, *Nucl. Phys.* **B415** (1994) 373; *Nucl. Phys.* **B335** (1990) 115;  
N. N. Nikolaev and B. G. Zakharov, *Z. Phys.* **C49** (1991) 607;  
H. G. Dosch and E. Ferreira, [hep-ph/0212257](#);  
J. Hufner, Y. P. Ivanov, B. Z. Kopeliovich and A. V. Tarasov, *Phys. Rev.* **D62** (2000) 094022;  
Y. P. Ivanov, J. Hufner, B. Z. Kopeliovich and A. V. Tarasov, [hep-ph/0212322](#).
- [19] M. G. Ryskin, R. G. Roberts, A. D. Martin and E. M. Levin, *Z. Phys.* **C76** (1997) 231;  
E. M. Levin, A. D. Martin, M. G. Ryskin, and T. Teubner, *Z. Phys.* **C74** (1997) 671.
- [20] L. Frankfurt, W. Koepf and M. Strikman, *Phys. Rev.* **D54** (1996) 3194; *Phys. Rev.* **D57** (1998) 512.
- [21] G. Kulzinger, H. G. Dosch and H. J. Pirner, *Eur. Phys. J.* **c7** (1999) 73;  
H. G. Dosch, T. Gousset, G. Kulzinger and H. J. Pirner, *Phys. Rev.* **D55** (1997) 2602.
- [22] J. Nemchik, N. N. Nikolaev, E. Predazzi and B. G. Zakharov, *Z. Phys.* **C75** (1997) 71;  
J. Nemchik, N. N. Nikolaev and B. G. Zakharov, *Phys. Lett.* **B341** (1994) 228.
- [23] Y. P. Ivanov, J. Hufner, B. Z. Kopeliovich and A. V. Tarasov, [hep-ph/0212322](#).
- [24] A. C. Caldwell and M. S. Soares, *Nucl. Phys.* **A696** (2001) 125.
- [25] H. G. Dosch, E. Ferreira and A. Kramer, *Phys. Rev. D* **50** (1994) [hep-ph/9405237](#).
- [26] J. Bartels, E. Gotsman, E. Levin, M. Lublinsky and U. Maor, [hep-ph/0212284](#).
- [27] ZEUS Collision, contribution No. 548 to the International Conference on High Energy Physics of the European Physical Society, 12-18 July 2001, Budapest, Hungary.
- [28] R.J. Eden, *"High Energy Collisions of Elementary Particles"*, Cambridge University Press (1967).
- [29] A.G Shuvaev, K.J Golec-Biernat, A.D Martin and M.G Ryskin, *Phys. Rev.* **D60** (1999) 014015;  
A. Freund and V. Guzey, *Phys. Lett.* **B462** (1999) 178.
- [30] H1 Collaboration, *Phys. Lett.* **B483** (2000) 23.
- [31] J. Pumplin, D. R. Stump, J. Huston, H. L. Lai, P. Nadolsky, W.K. Tung, [hep-ph/0201195](#).
- [32] H.A. Enge, *"Intr. to Nuclear Physics"*, Addison-Wesley Pub., Mass.,1971.
- [33] Atomic Data and Nuclear Data Tables, **14** (1974) 485.